International Journal of Mineral Processing 94 (2010) 115–120

Contents lists available at ScienceDirect

International Journal of Mineral Processing

journal homepage: www.elsevier.com/locate/ijminpro

Effect of frother on initial bubble shape and velocity

W. Kracht [a], J.A. Finch [b,*]

[a] Mining Engineering Department, Universidad de Chile, Av. Tupper 2069, Santiago, Chile
[b] Department of Mining and Materials Engineering, McGill University, 3610 University Street, Montreal, Quebec, Canada H3A 2B2

ARTICLE INFO

Article history:
Received 13 October 2009
Received in revised form 11 January 2010
Accepted 13 January 2010
Available online 21 January 2010

Keywords:
Bubble shape
Bubble rise velocity
Frothers

ABSTRACT

The effect of frother and NaCl salt on the shape and velocity of a ca. 2.4 mm diameter bubble close to the generation point at an orifice was studied using high-speed imaging. Bubbles accelerate to reach a maximum velocity at a given time depending on frother type and concentration, followed by deceleration and then oscillation about a mean velocity. A relationship between bubble shape and velocity is observed: the more spherical the bubble, the slower the rise, which is in agreement with recent literature. The findings support the argument that surfactants may affect bubble rise velocity through control of bubble shape.

1. Introduction

Frothers are surface-active agents (surfactants) widely used in flotation to aid generation of small bubbles. They also influence how bubbles move in a liquid (Frumkin and Levich, 1947; Dukhin et al., 1998). Clift et al. (2005), summarizing data spanning 70 years, show a decrease in rise velocity of single air bubbles over the size (diameter) range ca. 1 to 10 mm in water in the presence of so-called 'surface-active contaminants'. This effect is seen with frothers, recorded in the terminal velocity (Fuerstenau and Wayman, 1958; Zhou et al., 1992; Sam et al., 1996; Zhang et al., 1996) and the time history or velocity profile (Sam et al., 1996; Krzan et al., 2004). Azgomi et al. (2007) observed that, for a given gas rate, different frothers may generate the same gas holdup but with different bubble size, which suggests that bubble swarm velocity is affected by the presence of frothers. Zhou et al. (1993) made a similar claim. Acuna and Finch (2008) generating a 2D swarm confirmed this dependence on frother type.

These prior studies generally tracked bubble rise for at least one second. This communication shows the effect that common frothers (n-Pentanol, MIBC (methyl isobutyl carbinol), Dowfroth 250 (polyglycol ether), F-150 (polyglycol)) and salt (sodium chloride) have on bubble shape and rise velocity over the first ca. 0.4 seconds. The salt is included as high concentrations also act to reduce bubble size (Laskowski et al., 2003).

2. Bubble shape and rise velocity

Bubble motion may be classified into three regimes depending on rise velocity (Kulkarni and Joshi, 2005). The bubble Eötvös (Eo) and Reynolds (Re) numbers (Clift et al., 2005) are used in the characterization:

$$Eo = \frac{g(\rho_l - \rho_{air})d_{eq}^2}{\sigma} \quad (1)$$

$$\mathrm{Re} = \frac{\rho_l d_{eq} v}{\mu} \quad (2)$$

where g is the acceleration of gravity, ρ_l and ρ_{air} are the liquid and air density respectively, d_{eq} is the bubble equivalent spherical diameter, σ the surface tension, μ the liquid viscosity, and v the bubble rise velocity.

According to Tomiyama et al. (2002) the role of surfactants in the three regimes can be summarized as follows:

1. Viscous force dominant regime (small spherical bubble, Eo < 0.25): Accumulation of surfactant on bubble surface, together with the bubble motion, induces surface tension gradient effects that make the surface immobile and the bubble rise as a rigid sphere. The surface goes from free-slip to no-slip condition, resulting in an increase in viscous drag and decrease in terminal velocity. Bubbles under 1 mm in diameter are considered to be in this regime.
2. Surface tension force dominant regime (intermediate size bubble, 0.25 < Eo < 40): Surfactants reduce the shape oscillation, making bubbles more spherical. The terminal velocity becomes close to that of bubbles in clean systems with small initial shape deformation. Terminal velocity gradually decreases with increasing bubble size in this regime (the authors give a range of bubble sizes (1.3 mm–6 mm) based on a previous study (Peebles and Garber, 1953)). The bubbles in this study fall into this regime: 0.78 < Eo < 0.87 (210 < Re < 900).

* Corresponding author. Tel.: +1 514 398 1452; fax: +1 514 398 4492.
E-mail address: jim.finch@mcgill.ca (J.A. Finch).

0301-7516/$ – see front matter © 2010 Elsevier B.V. All rights reserved.
doi:10.1016/j.minpro.2010.01.003

3. Inertial force dominant regime (large bubble, Eo > 40): High inertia reduces the impact of surfactant in bubble motion and shape. The drag due to inertia is much higher than the viscous drag induced by surface tension gradient effects.

At Reynolds numbers higher than 200 (Re > 200), bubble buoyancy is complicated by bubble shape variation and bubble path instability (Dukhin et al., 1998). In a qualitative approach, it is suggested (Dukhin et al., 1998; Linton and Sutherland, 1957; Frumkin and Levich, 1947) that surfactants are swept to the rear of a rising bubble, generating a region of low surface concentration at the leading surface of the bubble and a region of large concentration at the rear pole of the bubble. The low concentration (leading) region remains mobile, whereas the high concentration (rear) region is characterized by retarded surface mobility (rear stagnant cap).

Finch et al. (2008) and Acuna (2007) studied the effect of surfactants (frothers) on single bubbles of ca. 3.5 mm diameter generated at a capillary tip over the first 50 ms or so. Bubbles blown in tap water and in surfactant solution (0.1 mmol/L polyglycol, F-150) behaved identically in terms of aspect ratio and local velocity over the first 10 ms following bubble detachment. After this the bubble in surfactant solution became more spherical than its water only cousin and slowed down significantly. The observation reveals that frother requires time to adsorb sufficiently to produce effects on bubble behavior; it takes time to establish the dynamic steady state structure of the adsorption layer on the rising bubble. Although over much shorter time periods, this finding is in agreement with others (Sam et al., 1996; Zhang et al., 2001; Krzan et al., 2004, 2007).

Krzan et al. (2004, 2007) studied local (instantaneous) velocities and shape variations of bubbles rising in presence of surfactants. They confirmed the previous findings of Sam et al. (1996) and Zhang et al. (2001, 2003) that after initial acceleration, bubbles either attained a constant velocity (terminal velocity) at high concentrations of surfactant, or passed through a maximum in the local velocity followed by a deceleration prior to reaching terminal velocity for low concentrations of surfactant. A variation in bubble shape was noted but not linked quantitatively to velocity other than to observe that bubble shape stabilized once terminal velocity was reached.

An impact on local rise velocity is not restricted to surfactant systems. Wu and Gharib (2002) produced spherical and ellipsoidal bubbles of equivalent volume in purified water and found that the spherical bubbles moved significantly slower than their ellipsoidal counterparts.

De Vries et al. (2002) studied the influence of bubble shape oscillations on local velocities of bubbles in the absence of surfactants. They found that shape oscillations correlated with an oscillating bubble rise velocity. The argument advanced was that the oscillations in velocity were caused by variations in the added-mass term, which corresponds to an inertia effect as the rising bubble has to push water out of the way. The virtual or added-mass term is taken into account to calculate the rate of exchange of momentum of objects (bubbles) accelerating, rotating or oscillating in fluids, which depends on the shape of the bubble (Kendoush, 2007).

From numerical analysis, Dijkhuizen et al. (2005) predicted oscillations in both shape and velocity of bubbles of 3 mm and larger in initially quiescent pure water. They considered the drag and virtual mass forces in their calculations.

The works of Wu and Gharib (2002), De Vries et al. (2002), and Dijkhuizen et al. (2005) therefore suggest it is bubble shape that controls velocity. The action of surfactant is then seen as one of modulating shape, making a bubble more spherical (due to surface tension gradient effects) that cause the bubble to slow down as opposed to the more direct effect of increasing drag due to surface tension gradient effects.

In this study, bubble shape and rise velocity over the first ca. 400 ms from release is examined in the presence of frothers and salt (NaCl). A strong correlation between shape and velocity is found.

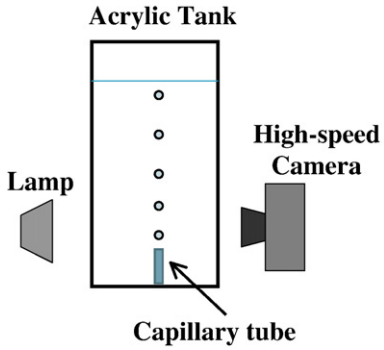

Fig. 1. Experimental set-up.

3. Experimental

3.1. Apparatus

The experimental set-up (Fig. 1) comprises a 30 L acrylic tank where air bubbles are injected through a glass capillary tube of 0.2 mm internal diameter. Gas flow rate is regulated by controlling the pressure in the line with a pressure regulator to generate a bubble growth rate of ca. 6.2 cm^3/min to produce bubbles of ca. 2.4 mm diameter (i.e., a growing time of ca. 70 ms). The tank is rear illuminated and bubbles are imaged with a high-speed camera (TroubleShooter HR) at a rate of 1000 frames per second and a resolution of 1280 × 512 pixels.

3.2. Reagents

Table 1 summarizes the reagents used. These represent the four classes of frothers from 'weakest' to 'strongest' as identified by Moyo et al. (2007): n-Pentanol, MIBC (methyl isobutyl carbinol), Dowfroth 250 (polyglycol ether), F-150 (polyglycol), and a member of the class of salts (sodium chloride) that at high concentration has the same effect on producing fine bubbles as frothers (Quinn et al., 2007). The HLB number (hydrophile–lipophile balance) is included as a scale of solubility of surfactant in water (Rao and Leja, 2004): the higher the HLB number the more water soluble (i.e., hydrophilic) is the reagent.

Solutions were made using Montréal tap water with temperature set at 20 °C, controlled by mixing warm and cold water. Between tests, the tank was emptied and carefully cleaned.

The frother concentrations employed cover the range of interest in flotation and were chosen based on the ability of these reagents to reduce bubble size in flotation cells (Nesset et al., 2007), hence the concentrations vary from frother to frother. As a guide to the concentrations used, Table 2 shows concentrations corresponding to a scale based on the critical coalescence concentration (CCC). In the table, the number accompanying CCC corresponds to the percentage of bubble size reduction compared to water alone (Nesset et al., 2007); CCC95, thus, corresponds to a concentration achieving 95% of bubble size reduction. For the case of sodium chloride, concentrations

Table 1
Summary of reagents used.

Reagent	Formula	Molecular weight (g/gmol)	HLB number	Supplier
n-Pentanol	$CH_3(CH_2)_4OH$	88.15	6.5	Fisher
MIBC	$(CH_3)_2CHCH_2CH(OH)CH_3$	102.18	6.1	Dow
Dowfroth 250[a]	$CH_3(PO)_4OH$	264.35	7.8	Dow
F-150[a]	$H(PO)_7OH$	425	8.5	Flottec
Sodium chloride	NaCl	58.44	–	Fisher

[a] PO is propylene oxide (propoxy) [–O–CH_2–CH_2–CH_2–].

Table 2
Typical frother concentrations (mmol/L) used in flotation systems expressed on CCC scale (adapted from Nesset et al., 2007).

Reagent	CCC50	CCC75	CCC95	CCC99
n-Pentanol	0.077	0.153	0.331	0.509
MIBC	0.026	0.051	0.111	0.171
Dowfroth 250	0.009	0.018	0.039	0.091
F-150	0.002	0.005	0.010	0.016

up to 1 mol/L were tested, based on the comparison between MIBC and salts made by Quinn et al. (2007).

3.3. The technique

Bubble shape and velocity were recorded with the high-speed camera over a distance of 85 mm from the capillary tip (a distance equivalent to 35 times the bubble diameter). Each video was processed off-line with ImageJ to yield bubble position, and dimensions (i.e., maximum and minimum diameter) vs. time. The position (x, y) was determined from the center point of the bubble, and the maximum and minimum diameters were determined by the best-fitted ellipse to the 2D-bubble image. The best-fitted ellipse is determined directly by the software, which also determines the angle between the maximum diameter and the y-axis (vertical axis). This allows not only calculation of the aspect ratio but whether the maximum or minimum diameter corresponds to the direction of movement of the bubble. The aspect ratio (A_R) is defined as the ratio between the diameters d_h and d_v, the diameters perpendicular and parallel to the direction of movement of the bubble respectively (Fig. 2):

$$A_R = \frac{d_h}{d_v} \tag{3}$$

The rise velocity (v) is calculated from the vertical position (y) of the bubble over two consecutive frames (i, $i+1$) as:

$$v = \frac{y_{i+1} - y_i}{\Delta t} \tag{4}$$

where Δt is the time interval between the two frames (1 ms).

The equivalent diameter (d_{eq}) is calculated assuming axial symmetry over the direction of movement:

$$d_{eq} = \left(d_v d_h^2\right)^{1/3} \tag{5}$$

For the purpose of this work, bubbles will be described as 'spherical' if the aspect ratio lies within 15% of unity ($A_R < 1.15$); otherwise, the bubble will be described as 'ellipsoidal'. Other bubble geometries, presented by Clift et al. (2005), are spherical-cap and ellipsoidal-cap, but these correspond to large bubbles (>10 mm) that tend to adopt flat or indented bases; these geometries were not observed in this study.

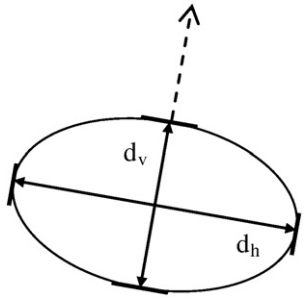

Fig. 2. Diameters d_h and d_v used to calculate the aspect ratio. The dashed arrow indicates direction of movement.

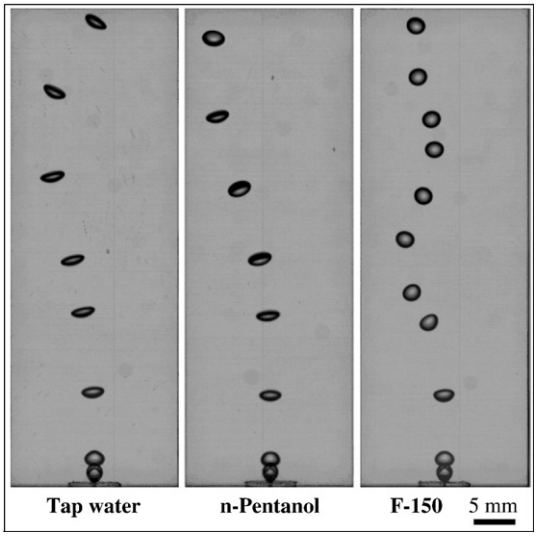

Fig. 3. Example of recorded images (taken from video each 30 ms). Tap water (no frother), n-Pentanol (0.40 mmol/L), and F-150 (0.012 mmol/L).

4. Results

The measurements, repeated 5 times for each condition, were consistent; for instance, for Dowfroth 250 (0.095 mmol/L), the pooled standard deviation for the aspect ratio, equivalent diameter, and velocity were 0.009, 0.01 mm, and 0.59 cm/s respectively.

4.1. Effect of frother type

Fig. 3 shows images of bubbles in tap water, in solutions of n-Pentanol (0.40 mmol/L) and F-150 (0.012 mmol/L) (i.e., equivalent concentrations on the CCC scale, Table 2). It is clear that F-150 has a dramatic effect on shape stabilization, whereas n-Pentanol has virtually no effect and is comparable to tap water. These three conditions are analyzed quantitatively by tracking the aspect ratio (shape) and local velocity with time after release.

Fig. 4 shows the results for the bubble in tap water. The velocity increases rapidly over the first ca. 40 ms, and then continues to slowly increase until ca. 150 ms, when it decreases followed by what seems to be an oscillating pattern around an average velocity of 30 cm/s. The reported bubble rise velocity for bubbles of 2.4 mm diameter in clean

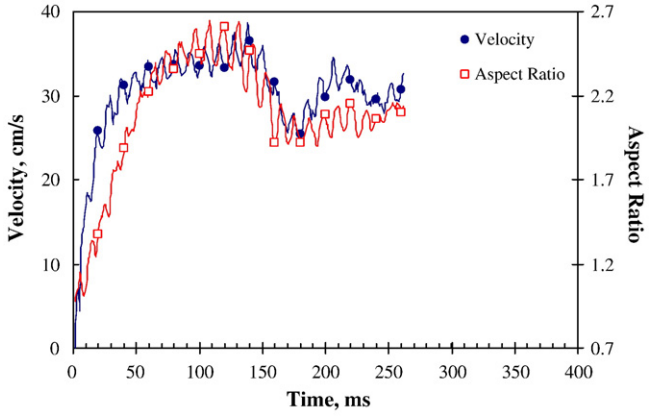

Fig. 4. Velocity and aspect ratio. Tap water. (Note symbols are used to identify the curves and have no other significance.)

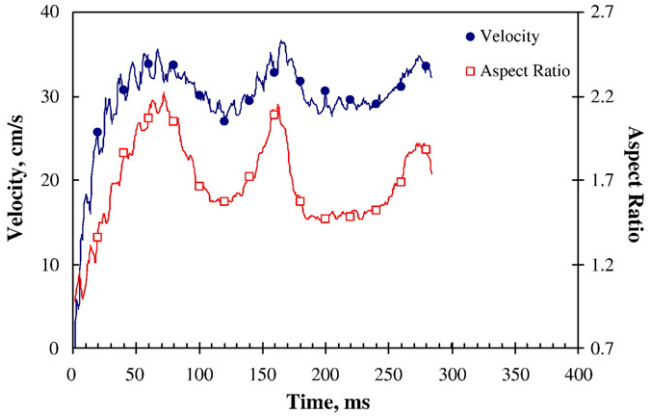

Fig. 5. Velocity and aspect ratio. n-Pentanol, 0.40 mmol/L.

water is ca. 28 cm/s (Clift et al., 2005). Note that the aspect ratio varies in accord with the velocity: the bubble leaves the capillary as a spherical object, but after ca. 10 ms it becomes ellipsoidal and retains that general shape ($A_R > 1.15$) for all other times.

As Fig. 3 reveals, at equal concentrations on the CCC scale frothers do not all have the same magnitude of effect on shape. Fig. 5 shows the quantitative results for n-Pentanol (0.40 mmol/L). The presence of this frother did not restore the spherical shape or reduce velocity significantly relative to water. The correlation between shape (aspect ratio) and velocity nevertheless remains.

Fig. 6, presents the significant impact that adding F150 (0.012 mmol/L) has on velocity and shape. In terms of shape, after detaching from the capillary as a spherical bubble ($A_R \sim 1$), the shape changes to ellipsoidal between ca. 10 and 70 ms, after which a spherical shape is reestablished, varying around a mean $A_R \sim 1.1$. The oscillations detected in water, and n-Pentanol, are damped in the presence of this frother. In terms of velocity, after accelerating for the first ca. 30 ms, the bubble reaches a maximum velocity of 30 cm/s, followed by deceleration to a minimum velocity of 10 cm/s prior to starting to oscillate about a mean of ca. 20 cm/s. (This velocity is below that in water and thus the bubble takes longer to reach the 85 mm height.) For a 2.4 mm diameter bubble in 'contaminated' water, Clift et al. (2005) give a velocity of ca. 17 cm/s. Observe that aspect ratio still oscillates in accord with the velocity.

The images in Fig. 3 suggest similar behavior regardless of conditions over the first few milliseconds (consider the first three bubble images). This is tested in Figs. 7 and 8, which show, respectively, the velocity and aspect ratio over the first 20 ms for tap water and at high concentration (>CCC95) of Dowfroth 250 (which is a 'strong' frother). No difference is observed in the velocity

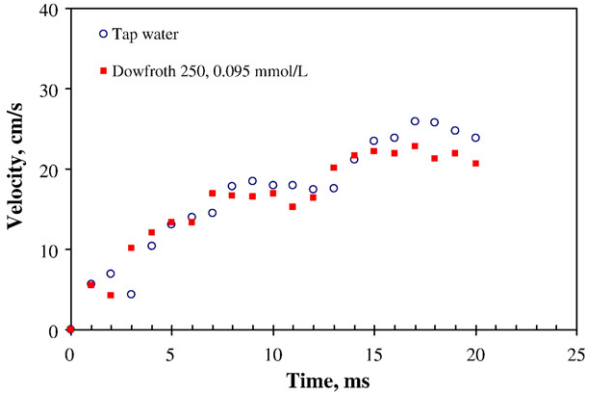

Fig. 7. Velocity over first 20 ms. Tap water; Dowfroth 250, 0.095 mmol/L.

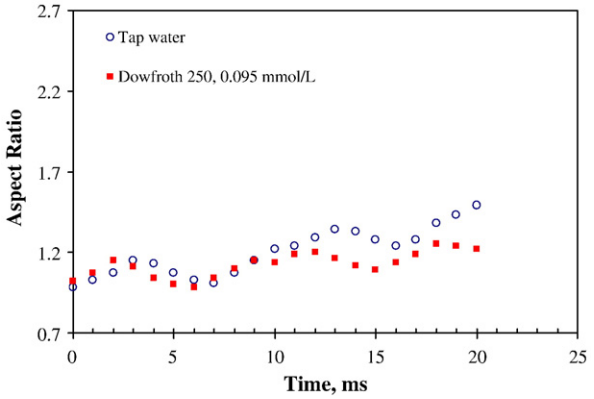

Fig. 8. Aspect ratio over first 20 ms. Tap water; Dowfroth 250, 0.095 mmol/L.

or aspect ratio over the first ca. 10 ms. The finding conforms with that of Acuna (2007).

4.2. Frother (MIBC) vs. salt (NaCl)

Quinn et al. (2007) showed that 10 ppm (0.098 mmol/L) MIBC gave similar bubble size distribution as 0.4 mol/L NaCl. Results for these two conditions are shown in Figs. 9 and 10 respectively.

Even though frother (MIBC) and sodium chloride exhibit different surface activity (frother positively adsorbs, salt negatively adsorbs), they give similar results: bubbles in both accelerate over the first 50 ms to reach a similar velocity and show oscillations in shape and velocity of similar frequency. Their effect is comparable to n-Pentanol.

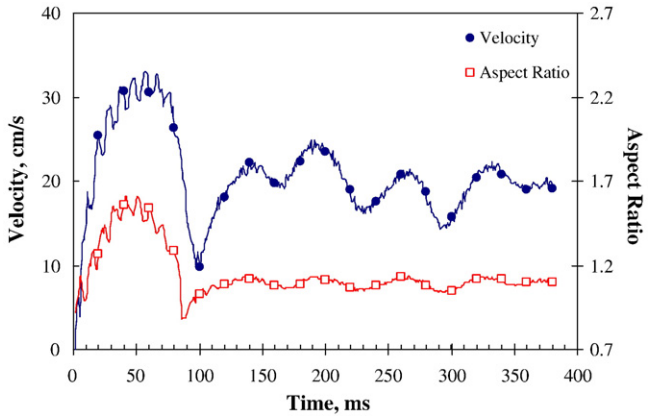

Fig. 6. Velocity and aspect ratio. F-150, 0.012 mmol/L.

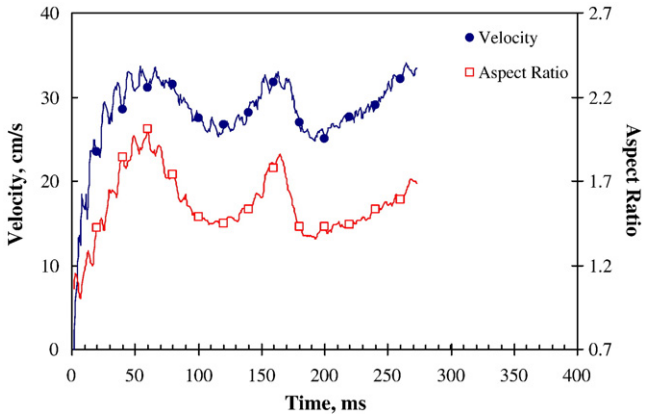

Fig. 9. Velocity and aspect ratio. MIBC, 0.098 mmol/L.

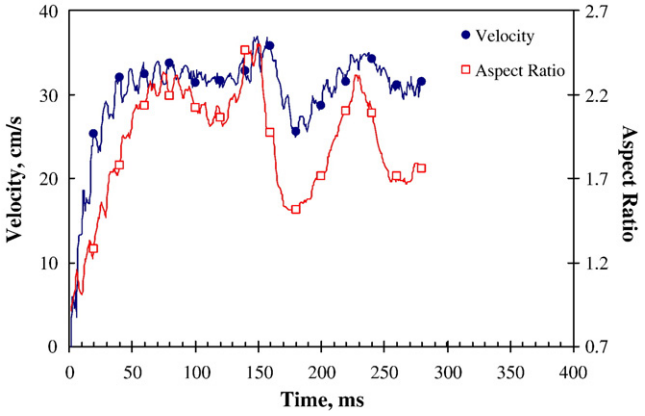

Fig. 10. Velocity and aspect ratio. NaCl, 0.4 mol/L.

4.3. Effect of frother concentration

Fig. 11 visualizes the effect on the bubble as frother (Dowfroth 250) concentration increases: the bubbles become more spherical and slow down (more bubbles in the frame).

Fig. 12 quantifies how the acceleration period and maximum velocity decrease as Dowfroth 250 concentration is increased. Subsequently, the oscillations appear to be similar in frequency and amplitude.

This shift in the first peak to shorter time was also observed with F150, another 'strong' frother but is not so evident for the other three reagents tested, Fig. 13 giving the example of MIBC. This is evidence of a weaker effect of these reagents on bubble shape stabilization.

4.4. General correlation of bubble rise velocity versus aspect ratio

The results indicate bubble shape varies in time in like manner as velocity. To explore, data were processed to yield the average velocity (and standard deviation) corresponding to each aspect ratio. Only data collected after the first deceleration period (i.e., where the bubble oscillates in shape and velocity) are considered. Fig. 14 shows the velocity versus aspect ratio for the maximum concentration tested for each reagent. The figure confirms a strong relationship between shape and bubble velocity: an increasing aspect ratio (bubbles more ellipsoidal) results in an increasing velocity with solution chemistry appearing to play only a secondary role.

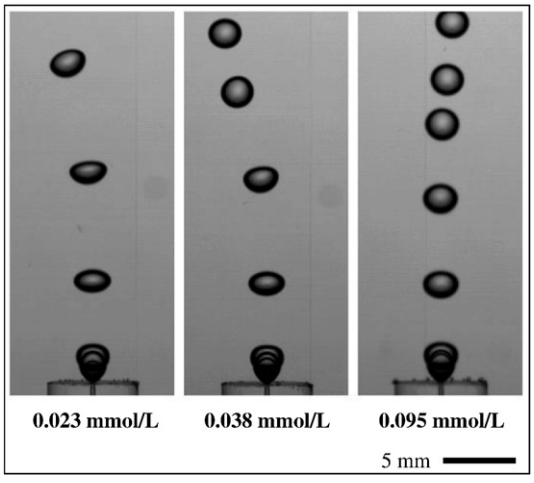

Fig. 11. Images showing impact of frother concentration (taken from video each 25 ms). Dowfroth 250.

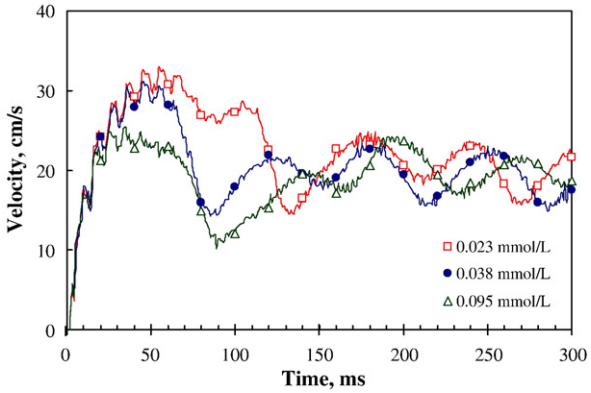

Fig. 12. Velocity as a function of frother concentration. Dowfroth 250: 0.023, 0.038, and 0.095 mmol/L.

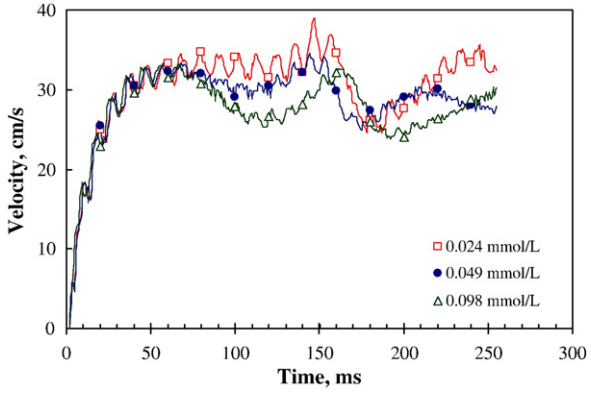

Fig. 13. Velocity as a function of frother concentration. MIBC: 0.024, 0.049, and 0.098 mmol/L.

5. Discussion

The experiments have shown that bubble shape and velocity are related: as shape becomes more spherical the bubble slows down and vice versa. The presence of frother stabilizes bubble shape, in particular eliminating the shape (aspect ratio) oscillation shown in water only. Bubble shape stabilization may be explained in terms of surface tension gradient driven phenomena (Gibbs elasticity and Marangoni effect) (Dukhin et al., 1998).

The impact on shape stabilization is not instantaneous as during the first 10–15 ms the results are the same regardless of the solution

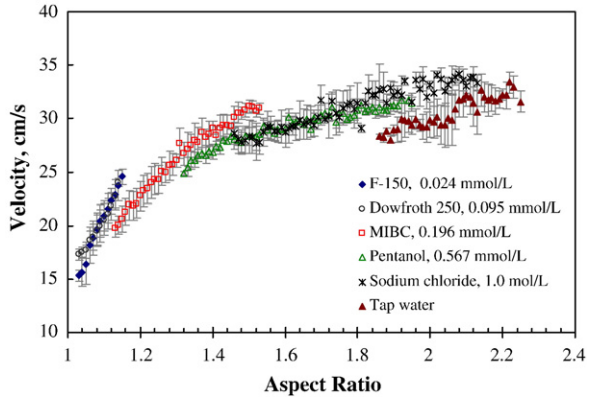

Fig. 14. Velocity vs. aspect ratio for maximum concentration tested: F-150, 0.024 mmol/L; Dowfroth 250, 0.095 mmol/L; MIBC, 0.196 mmol/L; n-Pentanol, 0.567 mmol/L; sodium chloride 1.0 mol/L; and tap water.

composition, i.e., it is the same as in water alone. This implies that time is needed to adsorb sufficient reagent to initiate the shape stabilization mechanism. Correlating with shape, bubbles show a maximum in velocity followed by a deceleration and then oscillation about a mean velocity.

De Vries et al. (2002) argued that bubble shape oscillations influenced bubble velocity as a consequence of variations in the added-mass which changes with bubble shape. The results here show that for all conditions there is a strong correlation between bubble shape (aspect ratio, A_R) and velocity. This behavior is typical of bubbles in the surface tension force dominant regime (Tomiyama et al., 2002). Over the concentration of interest in flotation (using the CCC criterion) Dowfroth 250 and F-150 proved to be strong bubble shape stabilizers; indeed both restore bubbles to spherical ($A_R < 1.15$) within 100 ms and produce the lowest rising velocities within the time frame measured. MIBC and n-Pentanol have less ability to restore spherical shape and consequently less impact on slowing the bubble (at least within the time frame explored here). This division corresponds to the classification 'strong' and 'weak' often employed to describe their relative frother action. In this respect, NaCl is also a weak 'frother'. The fact that all these reagents at the concentration used are capable of giving similar bubble size reduction in flotation systems but have these obvious differences in ability to control shape indicates that different mechanisms are involved in these two phenomena; the appeal to surface tension gradients as the source of shape control does not therefore appear to a factor in bubble size control.

The implication from recent literature is that bubble velocity depends on shape. Fig. 14 lends support to this primary effect of shape with system chemistry playing a secondary role on velocity. The findings support that an important role of surfactant (and salt) in modulating bubble velocity is through control of bubble shape in the surface tension dominant regime ($0.25 < Eo < 40$), one of the two cases relevant to flotation systems.

6. Conclusions

New findings are presented on the effect of frother and salt (NaCl) on bubble shape and velocity immediately after creation at an orifice (time < 400 ms). The results show no effect for the first ca. 10 ms after bubble detachment for any reagent tested. Bubbles reach different maximum velocities at different times depending on conditions. The maximum velocity is followed by a deceleration period and then oscillation about a mean velocity.

The oscillation in velocity is matched by oscillation in shape (aspect ratio). A relationship between bubble shape and velocity is observed: the more spherical the bubble, the slower it rises in agreement with Wu and Gharib (2002) who established this in the absence of surfactants. Dowfroth 250 and F-150 have a strong effect on stabilizing a spherical shape, and consequently produce the lowest bubble velocities. The other reagents tested, MIBC, n-Pentanol and NaCl, are less able to produce a spherical shape and consequently bubble velocity is higher. Nevertheless the correlation between shape and velocity is maintained.

The findings support the recent argument that surfactants, to which can now be added salts such as NaCl, affect bubble rise velocity primarily through control of bubble shape in the surface tension dominant regime ($0.25 < Eo < 40$).

Acknowledgements

Funding is under the Chair in Mineral Processing sponsored by Vale Inco, Teck Cominco, Xstrata Process Support, Agnico-Eagle, Barrick Gold, Shell Canada, SGS Lakefield, COREM and Flottec, through the NSERC (Natural Science and Engineering Research Council of Canada) CRD (Collaborative Research and Development) program.

W. Kracht would also like to thank the Chilean Government for the Chilean National Scholarship (Beca Presidente de la República) and Universidad de Chile for granting a leave and financial support.

References

Acuna, C., 2007. Measurement techniques to characterize bubble motion in swarms. McGill University, Montréal, QC, Canada. PhD Thesis.
Acuna, C., Finch, J.A., 2008. Motion of individual bubbles rising in a swarm. In: Wng, D., et al. (Ed.), Proceedings of XXIV International Mineral Congress, Beijing, Sept. 18–24, 2008, vol. 1, pp. 891–901.
Azgomi, F., Gomez, C.O., Finch, J.A., 2007. Characterizing frothers using gas hold-up. Canadian Metallurgical Quarterly 46 (3), 237–242.
Clift, R., Grace, J.R., Weber, M.E., 2005. Bubbles, Drops, and Particles. 2nd edition. Academic Press, New York.
De Vries, J., Luther, S., Lohse, D., 2002. Induced bubble shape oscillations and their impact on the rise velocity. The European Physical Journal B 29, 503–509.
Dijkhuizen, W., van den Hengel, E.I.V., Deen, N.G., van Sint Annaland, M., Kuipers, J.A.M., 2005. Numerical investigation of closures for interface forces acting on single air-bubbles in water using Volume of Fluid and Front Tracking models. Chemical Engineering Science 60, 6169–6175.
Dukhin, S.S., Miller, R., Loglio, G., 1998. Physico-chemical hydrodynamics of rising bubble. In: Möbius, D., Miller, R. (Eds.), Studies in Interface Science Vol. 6: Drops and Bubbles in Interfacial Research. Elsevier Science.
Finch, J.A., Nesset, J.E., Acuna, C., 2008. Role of frother on bubble production and behaviour in flotation. Minerals Engineering 21, 949–957.
Frumkin, A., Levich, V.G., 1947. On surfactants and interfacial motion. Zh. Fizicheskoi Khimii 21, 1183–1204.
Fuerstenau, D.W., Wayman, C.H., 1958. Effect of chemical reagents on the motion of single air bubbles in water. Transactions AIME 211, 694–699.
Kendoush, A.A., 2007. The virtual mass of an oblate-ellipsoidal bubble. Physics Letters A 366, 253–255.
Krzan, M., Lunkenheimer, K., Malysa, K., 2004. On the influence of the surfactant's polar group on the local and terminal velocities of bubbles. Colloids and Surfaces A: Physicochemical and Engineering Aspects 250, 431–441.
Krzan, M., Zawala, J., Malysa, K., 2007. Development of steady state adsorption distribution over interface of a bubble risitn in solutions of *n*-alkanols (C_5, C_8) and *n*-alkyltrimethylammonium bromides (C_8, C_{12}, C_{16}). Colloids and Surfaces A: Physicochemical and Engineering Aspects 298, 42–51.
Kulkarni, A.A., Joshi, J.B., 2005. Bubble formation and bubble rise velocity in gas–liquid systems: a review. Industrial and Chemical Engineering Research 44, 5873–5931.
Laskowski, J.S., Cho, Y.S., Ding, K., 2003. Effect of frothers on bubble size and foam stability in potash ore flotation systems. Canadian Journal of Chemical Engineering 81, 63–69.
Linton, M., Sutherland, K.L., 1957. Dynamic surface forces, drop circulation and liquid–liquid mass transfer. Second International Congress on Surface Activity, 1. Butterworth, London, pp. 494–501.
Moyo, P., Gomez, C.O., Finch, J.A., 2007. Characterizing frothers using water carrying rate. Canadian Metallurgical Quarterly 46, 215–220.
Nesset, J.E., Finch, J.A., Gomez, C.O., 2007. Operating variables affecting the bubble size in forced-air mechanical flotation machines. Proceedings of Ninth Mill Operators' Conference, Freemantle, WA, Australia, pp. 55–65.
Peebles, F.N., Garber, H.J., 1953. Studies on the motion of gas bubbles in liquids. Chemical Engineering Progress 49 (2), 88–97.
Quinn, J.J., Kracht, W., Gomez, C.O., Gagnon, C., Finch, J.A., 2007. Comparing the effect of salts and frother (MIBC) on gas dispersion and froth properties. Minerals Engineering 20, 1296–1302.
Rao, S.R., Leja, J., 2004. Surface Chemistry of Froth Flotation, Second Edition, Vol 2. Reagents and Mechanisms. Revised Edition. Kluwer Academic, New York, pp. 663–666. First Edition by Jan Leja.
Sam, A., Gomez, C.O., Finch, J.A., 1996. Axial velocity profiles of single bubbles in water/frother solutions. International Journal of Mineral Processing 47, 177–196.
Tomiyama, A., Celata, G.P., Hosokawa, S., Yoshida, S., 2002. Terminal velocity of single bubbles in surface tension force dominant regime. International Journal of Multiphase Flow 28, 1497–1519.
Wu, M., Gharib, M., 2002. Experimental studies on the shape and path of small air bubbles rising in clean water. Physics of Fluids 14 (7), L49–L52.
Zhang, Y., Gomez, C.O., Finch, J.A., 1996. Terminal velocity of bubbles: approach and preliminary investigations. In: Gomez, C.O., Finch, J.A. (Eds.), Proceedings of the International Symposium of Column Flotation, COLUMN'96, Aug. 26–28, Montréal, Québec, Canada, pp. 63–69.
Zhang, Y., McLaughlin, J.B., Finch, J.A., 2001. Bubble velocity profile and model of surfactant mass transfer to bubble surface. Chemical Engineering Science 56, 6605–6616.
Zhang, Y., Sam, A., Finch, J.A., 2003. Temperature effect on single bubble velocity profile in water and surfactant solution. Colloids and Surfaces A: Physicochemical and Engineering Aspects 223, 45–54.
Zhou, Z.A., Egiebor, N.O., Plitt, L.R., 1992. Frother effect on single bubble motion in a water column. Canadian Metallurgical Quarterly 31 (1), 11–16.
Zhou, Z.A., Egiebor, N.O., Plitt, L.R., 1993. Frother effects on bubble motion in a swarm. Canadian Metallurgical Quarterly 32 (2), 89–96.